3B2v7.51c GML4.3.1 NIMA : 41990 Prod.Type:COM pp.1–13(col.fig.:NIL) ED:VijayaT PAGN: CSR SCAN: ROOPKALA.G

ARTICLE IN PRESS

Available online at www.sciencedirect.com

SCIENCE DIRECT®

Nuclear Instruments and Methods in Physics Research A ▮ (▮▮▮▮) ▮▮▮–▮▮▮

NUCLEAR INSTRUMENTS & METHODS IN PHYSICS RESEARCH Section A

www.elsevier.com/locate/nima

A polarized target for the CLAS detector

C.D. Keith[a,*], M. Anghinolfi[b], M. Battaglieri[b], D. Branford[c], S. Bültmann[a,1], V.D. Burkert[a], S.A. Comer[d], D.G. Crabb[e], R. De Vita[b], G. Dodge[d], R. Fatemi[e], D. Kashy[a], S.E. Kuhn[d], Y. Prok[e], M. Ripani[b], M.L. Seely[a], M. Taiuti[b], S. Witherspoon[a]

[a] *Jefferson Laboratory, Thomas Jefferson National Accelerator Facility, 12000 Jefferson Avenue, Newport News, VA 23606, USA*
[b] *Istituto Nazionale di Fisica Nucleare, Sezione di Genova e Dipartimento di Fisica dell'Università, 16146 Genova, Italy*
[c] *Department of Physics and Astronomy, University of Edinburgh, Edinburgh EH9 3JZ, UK*
[d] *Department of Physics, Old Dominion University, Norfolk, VA 23529, USA*
[e] *University of Virginia, Department of Physics, Charlottesville, VA 22901, USA*

Received 11 October 2002; received in revised form 12 December 2002; accepted 10 January 2003

Abstract

We describe the design, construction, and performance of a polarized solid target for use in electron scattering experiments with the CEBAF Large Acceptance Spectrometer. Protons and deuterons are continuously polarized by microwave-induced spin–flip transitions at 1 K and 5 T. The target operated successfully during two cycles in 1998 and 2000, providing proton and deuteron polarizations as high as 96% and 46%, respectively. The unique features of the target which permit its use inside a 4π spectrometer are stressed. Comparison is made between the target polarization measured by the traditional method of NMR and by electron elastic scattering.

PACS: 29.25.Pj; 13.88+e

Keywords: Polarized target; Spin; Structure functions

1. Introduction

Polarization observables are fundamental tools for understanding the nucleon structure and for testing the basic principles of quantum chromodynamics. Measurements of such observables have been successfully performed at several facilities during the last decades. The spin structure functions g_1 and g_2 in the deep-inelastic scattering regime have been measured at SLAC, CERN, and DESY using polarized electron and muon beams and polarized proton and deuteron targets (for a recent review see Ref. [1]). Polarized photon beams are used with polarized targets at both Mainz and Bonn to investigate the spin structure of the nucleon resonances and to test the Gerasimov–Drell–Hearn sum rule [2,3]. Nevertheless the

*Corresponding author. Tel.: +1-757-269-5878; fax: +1-757-269-5800.
E-mail address: ckeith@jlab.org (C.D. Keith).
[1] Present address: Brookhaven National Laboratory, Upton, NY 11973-5000, USA.

0168-9002/03/$ - see front matter
doi:10.1016/S1350-9462(02)00045-9

existing measurements do not yet provide a complete mapping of these observables, and more data are needed as a basis of new theoretical developments.

The EG1 experimental program in Hall B at the Thomas Jefferson National Accelerator Facility utilizes polarized electron scattering from polarized protons and deuterons to measure spin observables in the nucleon resonance region both from inclusive ($\vec{e}\vec{N} \to e'X$) and exclusive scattering ($\vec{e}\vec{N} \to e'N'\pi$).[2,3,4,5] To cover this broad physics program a dual NH_3/ND_3 target, polarized via the method of Dynamic Nuclear Polarization (DNP), has been constructed. The system, based on a 5 T superconducting magnet and a 1 K ^{4}He refrigerator, was realized by a collaboration of the Italian Istituto Nazionale di Fisica Nucleare, Jefferson Laboratory, Oxford Instruments,[6] and the University of Virginia.

In the following article, the design and performance of the target will be described. In Section 2 a brief review of the DNP technique is presented. Detailed descriptions of the polarized target system and its various components are given in Section 3. Particular emphasis is given to the unique constraints placed upon the target by the EG1 experiments. The performance of the target during these experiments is reviewed in Section 4.

2. Dynamic nuclear polarization

DNP is a well-established technique that is used to produce polarized targets for nuclear and particle physics experiments. The fundamental principles of DNP have been thoroughly reviewed by Abragam and Goldman [4] while Crabb and Meyer [5] describe the use of dynamically polarized solid targets in recent experiments. In this section, we give a brief sketch of the technique using the so-called ''well-resolved solid effect''. While the solid effect is not directly applicable to substances where the ESR linewidth is appreciably broadened (such as paramagnetically doped ammonia), it nevertheless contains the essential details of DNP: electronic spin flips, induced by microwave irradiation, are accompanied by nuclear spin flips which result in a net polarization of the nuclear spins. A more accurate but less intuitive description is provided by spin temperature theories of the process [4].

To realize DNP, a hydrogenated or deuterated compound is doped with paramagnetic radicals, usually in the form of unpaired electron spins at a relatively low concentration ($\sim 10^{-4}$). The compound is cooled to a low temperature and placed in a high magnetic field. A field-to-temperature ratio of five tesla/kelvin or greater is desirable for achieving the highest degree of nuclear polarization. Under these conditions the polarization of the free electron spins approaches unity. Microwaves of frequency near the electron spin resonance are then used to induce transitions which flip both the spin of the electron and that of a nearby proton (or deuteron).

The electron spins relax back to the lower energy spin state quickly ($\sim 10^{-3}$ s) due to the strong coupling between the electrons and the lattice. Once in the lower energy state, the electrons are again available to perform spin–flips with additional nuclei. As the nuclear spins couple weakly with the lattice, their spin-relaxation rates are much longer ($\sim 10^{3}$ s). The nuclei near the free electrons thereby accumulate into one spin state, which can be selected by the proper microwave frequency. The result is a net nuclear polarization which propagates throughout the bulk of the sample due to direct spin-exchange interactions between the nuclei (spin diffusion).

For the EG1 experiments, ammonia ($^{15}NH_3$ or $^{15}ND_3$) was chosen as the sample material. Proton (deuteron) polarizations in excess of 90% (40%) have been achieved in this compound, which provides a relatively high percentage of polarizable nucleons per total number of nucleons (16.7% for $^{15}NH_3$ and 28.6% for $^{15}ND_3$). In addition, ammonia has shown a high resistance to radiation

[2] JLab E91-023, Spokespersons V.D. Burkert, D.G. Crabb, R. Minehart.

[3] JLab E93-009, Spokespersons S.E. Kuhn, G.E. Dodge, M. Taiuti.

[4] JLab E93-036, Spokespersons M. Anghinolfi, R. Minehart, H. Weller.

[5] JLab E94-003, Spokespersons P. Stoler, R. Minehart, M. Taiuti.

[6] Oxford Instruments, Tubney Woods, UK.

damage that has restricted the use of most other polarizable materials to low luminosity or neutral-particle beam experiments [5]. The nitrogen nuclei are polarized by the DNP process along with the free protons and deuterons. For this reason, enriched ^{15}N (99%) is preferred over ^{14}N because most of the ^{15}N spin is carried by a single valence proton. This simplifies corrections to the scattering asymmetries due to the presence of polarized background material.

Paramagnetic radicals are produced in the ammonia by subjecting the material (in the form of 1 mm frozen granules) to ionizing radiation. The initial dose of radiation was applied at temperatures near 80 K using either the 20 MeV electron beam of the Stanford University SUNSHINE facility or the 38 MeV electron beam of the TJNAF Free Electron Laser. The total electron charge applied to the material was approximately 10^{17} electrons/cm^2. The irradiated material is then stored in a liquid nitrogen dewar until its use in the polarized target.

Additional irradiation at 1 K during the scattering experiment eventually produces an overabundance of paramagnetic radicals that prove detrimental to the polarization process. These radicals are removed by periodically annealing the sample at 80–100 K for up to 1 h, thus restoring the polarization to its initial value. In the case of deuterated ammonia the annealing process can result in a polarization that often exceeds the initial value.

3. The polarized target system

The wide physics program covered by this experiment and the unique features of the Hall B detector system have introduced severe constraints on the target design and optimization. Experiments involving polarized targets have traditionally used small solid-angle spectrometers located relatively far from the target, thus resulting in negligible interference between the two systems. In such cases it is possible to use continuously polarized targets, which often contain two or more samples at the same time. A few targets, based on the "frozen spin" concept [5], have operated in conjunction with large acceptance detectors. These provide only a single sample however, and require that data acquisition be periodically halted while the sample is repolarized.

The target described here is continuously polarized, allows the user to select between four different samples, and is designed to fit *inside* the CEBAF Large Acceptance Spectrometer (CLAS) [6]. The latter is a multigap magnetic spectrometer in which the field is generated by six superconducting coils arranged in a toroidal configuration. The regions between the torus coils are individually instrumented to comprise six independent spectrometers, providing an angular coverage of nearly 4π. This configuration leaves a magnetic field-free region in the center of the detector that is well suited for the insertion of a polarized target.

The target system must still satisfy stringent constraints due to the limited size of the field-free region and the impact of the polarizing magnet on both the scattered particle trajectories and detector background produced by Møller-scattered electrons. Most importantly, the target design must provide the large angular acceptance necessary to detect exclusive final states.

A side-view of the polarized target system positioned inside CLAS is shown in Fig. 1, while Fig. 2 provides a closeup view of the target itself. The various subsystems which comprise the target are the superconducting magnet, the 1 K refrigerator, the microwave and NMR systems, and the sample insert. Each of these is described separately in the following subsections. The entire assembly, including the pumping system, is attached to a rail-mounted cart that can be rolled into and out of CLAS in a matter of minutes.

3.1. Superconducting magnet

The superconducting Helmholtz magnet produces a 5 T field parallel to the electron beam axis. At its center, the field is uniform to better than 1×10^{-4} over a cylindrical volume 20 mm in diameter and 20 mm long. This uniformity is necessary to resolve the ESR linewidth of the paramagnetic radicals responsible for the DNP process. The center of the magnet is positioned

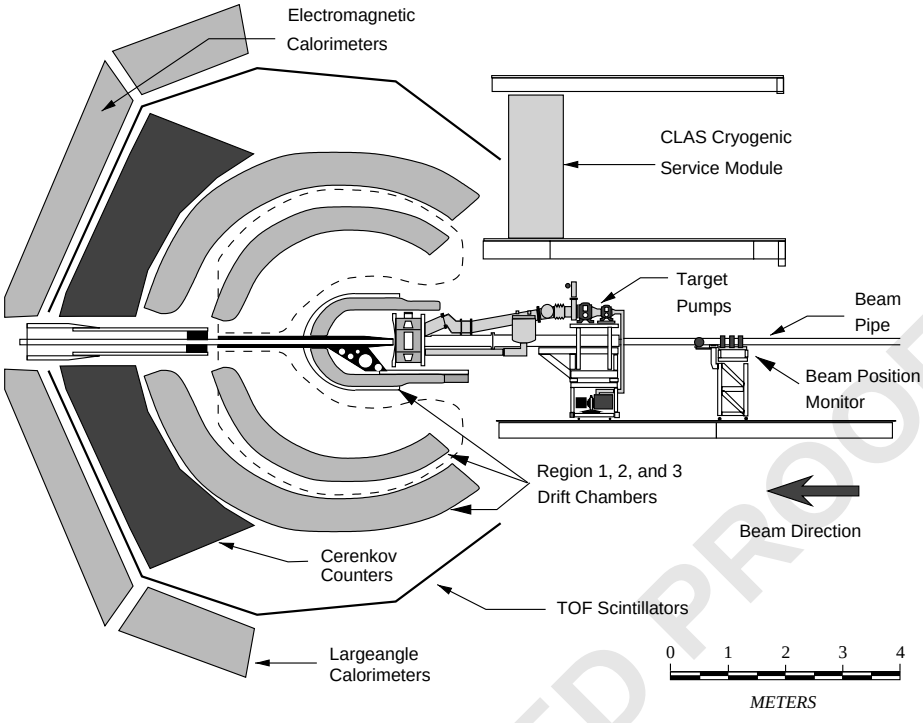

Fig. 1. Schematic view of the polarized target positioned inside the CLAS detector system. Two of the spectrometer's six superconducting coils (which are not visible in this sectional drawing) are outlined by the dashed lines.

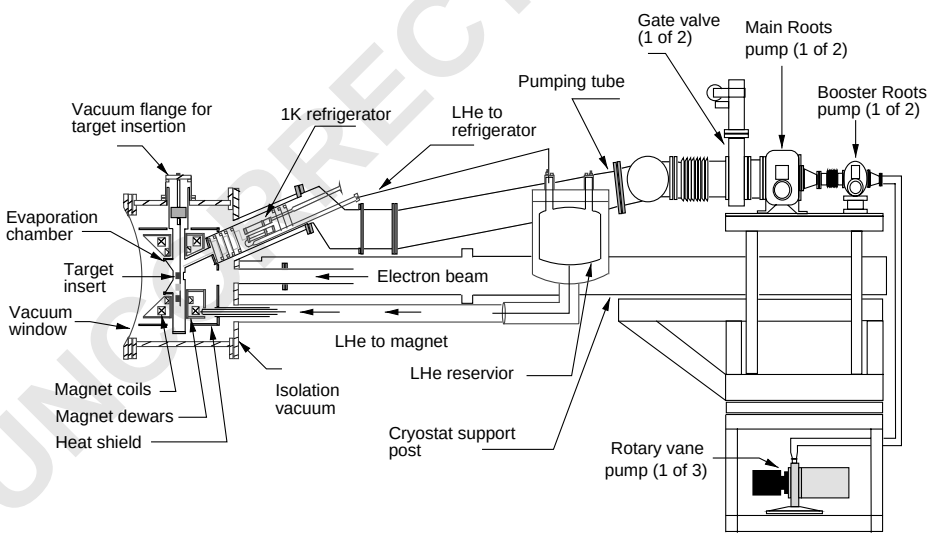

Fig. 2. Cutaway view of the polarized target cryostat from the beam-left side.

570 mm from the center of the CLAS detector. In this position the target's magnetic field serves as an effective focusing magnet for Møller-scattered electrons, thus reducing the detectors' background counting rates.

The on-axis bore of the magnet is 200 mm in diameter, and provides a $\pm 50^{\circ}$ open aperture for particles scattered in the forward (downstream) direction. In the upstream direction, the large bore of the magnet accommodates access for both the electron beam pipe and the 1 K refrigerator. Each coil is encased in a stainless steel dewar with four interconnecting tubes between the two. The gap between the coil packages is 80 mm, providing an aperture for particles scattered 75–105° in the azimuthal direction. The magnet requires approximately 60 min to ramp to 5 T and is operated in persistent current mode to ensure field stability and to reduce the liquid helium consumption.

The magnet dewars are rigidly suspended from the upstream end of the outer vacuum chamber and are cooled to 4.2 K via a 2 m long, vacuum-insulated pipe that connects to a liquid helium reservoir located outside CLAS. There are no penetrations into the magnet dewars except through this pipe, thus reducing potential damage to the detector from the exhaust of cold gas during a magnet quench. The total volume of LHe contained in the reservoir and magnet dewars is 25 l. This liquid is periodically replenished from a 500 l LHe dewar which is in turn replenished by the TJNAF End Station Refrigerator.

Due to the space constraints imposed by CLAS, there is no liquid nitrogen shield surrounding the magnet dewars. Instead, the boil-off from the dewars is used to cool a cylindrical aluminum heat shield surrounding the coils. To minimize the energy loss experienced by scattered particles, six lateral holes have been cut from the heat shield, each hole corresponding to one of the six regions of the CLAS detector. The holes are covered by only a few layers of aluminized mylar super-insulation. The downstream end of the heat shield is likewise covered by only a few layers of super-insulation.

A single vacuum vessel provides vacuum insulation for both the magnet dewars and liquid helium reservoir. At the magnet end, this vacuum can is a hexagonal prism, axis aligned parallel to the electron beam, with six lateral windows mimicking the geometry of the CLAS detector. The lateral windows are constructed from 0.13 mm thick aluminum, while the downstream axial window is 700 mm in diameter and is constructed from 0.28 mm thick aluminum. The central portion of this window is made of 0.07 mm thick aluminum to allow the primary, unscattered electron beam to exit.

The evaporation rate of LHe from the EG1 magnet and reservoir dewars is about 5 l/h, implying a heat load of approximately 3.5 W. This results from compromises made in the thermal shielding of the magnet and the unusually large exit windows for scattered particles. A polarized target which has operated both at SLAC and in Hall C at Jefferson Lab [7] utilizes a superconducting magnet of similar design (but with smaller exit windows and a LN2 shield) and displays a boil-off rate of less than 1 l/h.

3.2. Refrigerator

The polarized target material is maintained at a temperature of approximately 1 K by immersion into a pumped bath of liquid ^{4}He. A cooling power of about 0.8 W is achieved at 1.1 K with a system of Roots and rotary-vane vacuum pumps that provide a pumping speed for helium of 3300 m^3/h.

The evaporation chamber is situated at the center of the superconducting Helmholtz coils and consists of a stainless steel hexagonal prism of 500 mm circumference and 70 mm length. Like the outer vacuum can, the chamber has six lateral windows (50 μm thick stainless steel) arranged to mimic the geometry of CLAS. The electron beam entrance window (71 μm thick, 21 mm diameter aluminum) and refrigerator pumping tube are located on the up-stream end of the chamber, while the forward-scattered particles exit through a 71 μm thick window (42 mm diameter) on the downstream end.

Liquid helium is supplied to the evaporation chamber through a refrigerator that is similar to that originally used by Roubeau [8]. The refrigerator is inserted into the 200 mm diameter pumping tube between the LHe evaporation chamber and the Roots pumps and receives LHe from the same reservoir that services the superconducting magnet. The liquid first enters a copper pot where the remaining vapor is pumped away. Liquid from this separator pot drains into the

evaporation chamber through a 2.5 mm copper tube heat sunk to a series of seven perforated copper plates. The plates act as liquid–gas heat exchangers between the incoming liquid and the vapor pumped from the evaporation chamber. The perforations are 1 mm in diameter with a 2 mm spacing. The flow of liquid through the heat exchangers is metered by a remotely controlled needle valve. A second needle valve is used to bypass the heat exchangers during the initial cooling process.

The traditional approach to polarized solid targets has been to orient the refrigerator in either the vertical or horizontal direction. Space constraints inside the CLAS detector eliminate the possibility of using a vertical refrigerator, while a horizontal design precludes the rapid change from one target sample to another. Therefore this refrigerator is tilted at an angle of 25° from the horizontal, while the target samples are loaded vertically into the evaporation chamber through a separate tube.

The cooling power of this refrigerator, measured with a resistive heater in the evaporation chamber, is shown in Fig. 3. The temperature was determined using a ^{3}He vapor pressure thermometer. The solid curve in the figure is the ideal cooling power of the LHe evaporation process assuming a pumping speed of 3300 m^3/h. From the figure we can estimate a background heat load of approximately 0.4 W. There are four major sources of heat to be considered.

First, the beam-exit and radial surfaces of the evaporation chamber are poorly shielded against thermal radiation. Assuming a radiation shield temperature of 100 K and a thermal emissivity of 0.1 for stainless steel results in a radiative transfer of about 0.04 W. However, any improvement in the radiation shielding would compromise the acceptance of scattered particles.

Second, the refrigerator pumping tube and target insertion tube each provide a path for thermal conduction. While the pumping tube is efficiently cooled by the flow of cold helium gas, the insertion tube is not, and contributes about 0.18 W of conductive heat transfer. The column of helium gas in this tube adds an additional 0.05 W.

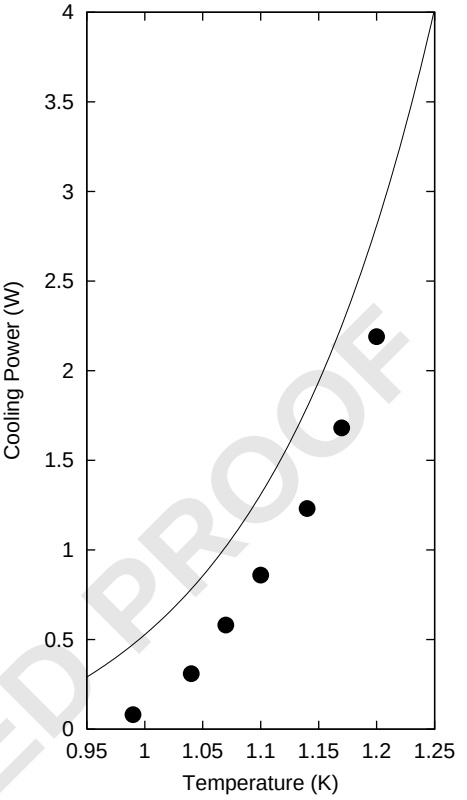

Fig. 3. Measured cooling power of the 1 K refrigerator as a function of the evaporation chamber temperature (●). The solid line is the calculated cooling power for the refrigerator assuming no external heat load.

Third, both the insertion tube and pumping tubes are susceptible to superfluid film creep. The flow rate of the superfluid film is difficult to estimate since it depends strongly on the surface condition of the tube. White reports a flow rate of $\dot{V} \simeq 7 \times 10^{-5} S$ cm^2 s^{-1} for a clean glass tube of perimeter S, and a rate about ten times higher for typical metal surfaces [9]. The latter would correspond to the evaporation of about one gas liter (STP) per minute in this refrigerator, which would appear as a 0.07 W load. In principle, the film creep could be suppressed by inserting small, 1 mm diameter orifices in its path, but of course such orifices would block the insertion of both the polarized target material and the microwave waveguide.

Finally, we consider the heat exchange between the incoming liquid helium and outgoing helium vapor. Under normal conditions the temperature of the last heat exchanger is about 1.2 K for a molar flow rate of 0.02 mol s^{-1}. The difference in enthalpy for LHe between 1.0 and 1.2 K is about 4 J/mol, leading to a head load of 0.08 W from the incoming liquid.

The total for the four sources considered is 0.42 W, close to the observed value. More than half of this heat load comes from conduction through the insertion tube. In a traditional target design, the target is inserted *through* the pumping tube, and this source of heat is eliminated.

3.3. Target insert

The target material is supported in the 1 K helium bath by an insert that can be introduced into the evaporation chamber through a port located at the top of the vacuum can. The insert, shown in Fig. 4, consists of a thin aluminum structure and four cells that contain the target material. For thermal isolation, a teflon block separates the upper portion of the insert from the lower.

A hydrogen-free plastic, polychlorotrifluoroethylene (PCTFE), was chosen for the cell walls because it does not produce a NMR background signal at the proton Larmor frequency and because its resistance to radiation damage is superior to that of the more common hydrogen-free plastics such as teflon. The cell dimensions (10 mm in length and 15 mm in diameter) were determined by the limitations imposed by multiple scattering and by the maximum luminosity acceptable by CLAS. The thicknesses of the cell walls (0.2 mm), aluminum entrance windows (25 μm), and kapton exit windows (50 μm) were minimized to reduce the energy loss of scattered particles.

The insert is thermally grounded near its top to a brass disk that is in turn thermally grounded to the heat shield of the magnet. This disk is also used to heat sink instrumentation wiring and NMR cables. The disk is connected to the top flange by a threaded stainless steel rod. This rod is attached via a vacuum-tight seal to a remotely controlled stepping motor that allows each of the four cells to be moved onto the electron beam axis with a vertical precision of 2 μm. Moving from one cell to the next requires about 1 min. A set of rails, between the evaporation chamber and the top flange, is used to maintain the horizontal alignment of the target cells.

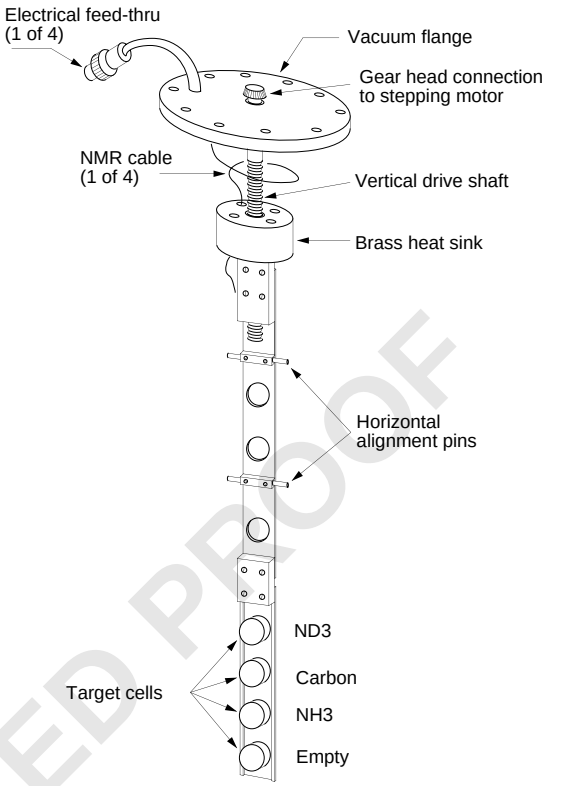

Fig. 4. Sample insert for the polarized target material. The NMR coils wrapped around the NH_3 and ND_3 cells are not drawn.

During operation, two of the four target cells are filled with $^{15}NH_3$ and $^{15}ND_3$ for the physics measurements. The remaining two cells are utilized for background studies and systematic checks. One of these cells is filled with a 2.3 mm thick carbon disk, while the other is left empty. With this design a complete series of measurements on both polarized protons and polarized deuterons, along with the accompanying background measurements, can be accomplished without the time-consuming replacement of target material. A separate insert, described below, is necessary for

cross-calibration between the carbon disk and the ^{15}N contained in the solid ammonia samples.

Due to the limited dimensions of the cells, the NMR coils are located on the outside of the PCTFE cells. Their geometry has been optimized to provide maximum sensitivity to the target polarization and its uniformity. The coils consist of thin-walled CuNi tubing (0.55 mm diameter) bent into a rectangular shaped loop. This loop is then wrapped around the outside of the cell to subtend an angle of 150–180°. One loop is sufficient to detect the thermal-equilibrium polarization signal of protons in NH_3. The inductance of the ND_3 coil must be increased in order to compensate for the deuteron's lower Larmor frequency, and here we use four loops superimposed two-by-two and mounted on opposite sides of the cell. A third single-loop coil, wrapped around the NH_3 cell, is used to measure the polarization of ^{15}N nuclei in the sample. A fourth coil is wrapped around the ND_3 cell in order to measure the polarization of residual protons in that material. The NMR electronics are described in Section 3.5.

Four cryogenic coaxial cables connect the coils to the upper flange. Temperature sensors are located at various positions on the insert to monitor the material condition during the target operations. Annealing the target material is accomplished by wire-wound heaters mounted directly below each cell while thermocouples located inside the cells are used to measure the temperature of the material during the process.

A second insert is used for background studies on solid ^{15}N. This insert consists of a Torlon cell (15.7 mm diameter, 12.7 mm long) sealed at both ends by kapton foil. Isotopically enriched (98%) ^{15}N gas is introduced into the cell from a room temperature gas handling system via a pair of 2.4 mm stainless steel tubes. The insert is loaded into the evaporation chamber and ^{15}N condenses inside the cell as the chamber is cooled and filled with LHe. Manganin heater wire is wrapped around the fill tubes to prevent them from plugging with solid nitrogen before the cell is completely filled. A 2.2 mm thick carbon disk is situated beneath the nitrogen cell and is used for cross-calibration of the ^{15}N and carbon backgrounds. The ^{15}N insert has proven particularly valuable. It has allowed experimenters, for the first time, to extract the dilution due to unpolarized nucleons in ammonia without any need for nuclear structure models or cross-section corrections.

3.4. Microwave system

The microwave field necessary to polarize the target material is generated by an Extended Interaction Oscillator[7] (EIO) capable of several watts of power at 140 GHz with a linewidth of about 10 MHz. Typically about 1 W is delivered to the target. The center frequency may be varied by mechanically adjusting the length of the resonant cavity using a remotely controlled DC motor. The tube can be tuned over a bandwidth of 2 GHz, which allows us to polarize the targets into either the positive or negative spin state (separated by approximately 400 MHz at 5 T) without reversing the magnetic field.

The microwave frequency is measured with an EIP model 588C frequency counter, and the tube power is monitored by a temperature-compensated thermistor read by a HP model 432 power meter. The microwaves are transmitted to the target through rectangular WR-6 waveguides outside the cryostat, and through a 5 mm CuNi tube inside. A 0.1 mm thick piece of FEP film is used to make a vacuum tight seal between the CuNi tube and a rectangular-to-round waveguide adapter. The CuNi tube enters the evaporation chamber via the central axis of the refrigerator pumping tube and terminates with a gold-plated rectangular horn. The horn is rigidly fixed inside the chamber and is oriented so as to broadcast microwaves at whatever target is on the electron beam axis.

3.5. NMR system

Continuous wave NMR is used as an online monitor of the NH_3 and ND_3 polarizations. The NMR system is designed around the Liverpool Q-meter circuit [10] and is sketched in Fig. 5. Briefly, the NMR coil is wrapped around the polarized target material and forms part of a resonant RLC

[7] CPI, Canada, Model VKT2438P5.

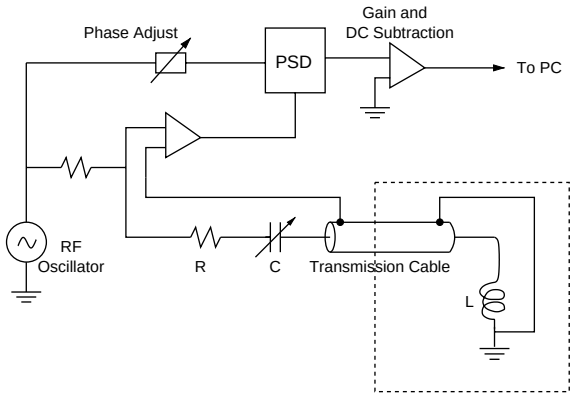

Fig. 5. Schematic drawing of the NMR electronics. The portion inside the dashed box is located inside the target cryostat.

circuit. As the RF driving frequency is swept at a constant current through the nuclear Larmor frequency, the resulting spin flips alter the nuclear susceptibility of the sample. This is observed as a change in the complex impedance of the circuit. The real part of the voltage dropped across the circuit is measured with a phase-sensitive detector by mixing this signal with a reference signal of the same frequency.

The RF frequency is swept through the proton (deuteron) Larmor frequency of 212.6 MHz (32.6 MHz) with a sweep width of about 0.4% (0.2%). The sweep is performed from lower to higher frequency and then reversed. A preset number of these "double" sweeps are accumulated and averaged before the polarization is calculated. The frequency is generated by a PC-controlled RF signal generator,[8] and the output voltage of the Q-meter[9] is recorded by a multi-purpose data acquisition board.[10]

In a plot of voltage versus frequency, the polarization of the sample is proportional to the area under the curve. Unfortunately, the constant of proportionality depends on several circuit and sample parameters and is difficult to calculate accurately. It is instead determined by measuring the NMR signal corresponding to a known, thermal equilibrium polarization. This is typically done at 1.6 K where the proton (deuteron) polarization is 0.319% (0.065%) in a 5 T field. The temperature is determined using both a ^{3}He vapor pressure bulb located inside the evaporation chamber and by measurement of the ^{4}He vapor pressure inside the chamber itself. Typical NMR signals for the proton and deuteron are displayed in Fig. 6.

The ND_3 signal has two peaks due to the interaction of the deuteron's electric quadrupole moment with electric field gradients within the material. This interaction produces an asymmetric splitting of the $2I+1$ magnetic substates, thus the maxima of the $1 \leftrightarrow 0$ and $0 \leftrightarrow -1$ NMR transitions occur at different frequencies. The deuteron vector polarization can be estimated using the relative heights of the two peaks [11]

$$P_d = \frac{r^2 - 1}{r^2 + r + 1} \quad (1)$$

where $r = A/B$ is the ratio of the two transition strengths, and A and B are indicated in Fig. 6. This peak-height method of determining the polarization is subject to non-negligible corrections that arise from the off-resonance response of the NMR circuit. The results of Ref. [11] however, indicate that for deuteron polarizations greater than about 20% an accuracy of 2–3% can be realized.

The relative accuracy of polarizations obtained via thermal equilibrium calibrations is typically 3% in the case of the proton and only about 8% for the deuteron. In both cases the uncertainty is dominated by nonstatistical fluctuations in the thermal equilibrium measurements. These fluctuations are the result of thermal drifts in the NMR circuit both inside and outside the target cryostat and are more problematic for the smaller deuteron signal. For this reason, the peak-height method was the primary method of deuteron polarimetry during most of the EG1 data taking.

3.6. Comparison of NMR with elastic scattering asymmetries

An additional method for determining the target polarization is to measure the elastic (quasi-elastic) scattering of polarized electrons from the polarized proton (deuteron) target. This technique can

[8] Rohde and Schwartz SMT02.
[9] Ultra Physics Ltd.
[10] National Instruments PCI-MIO-16IE-10.

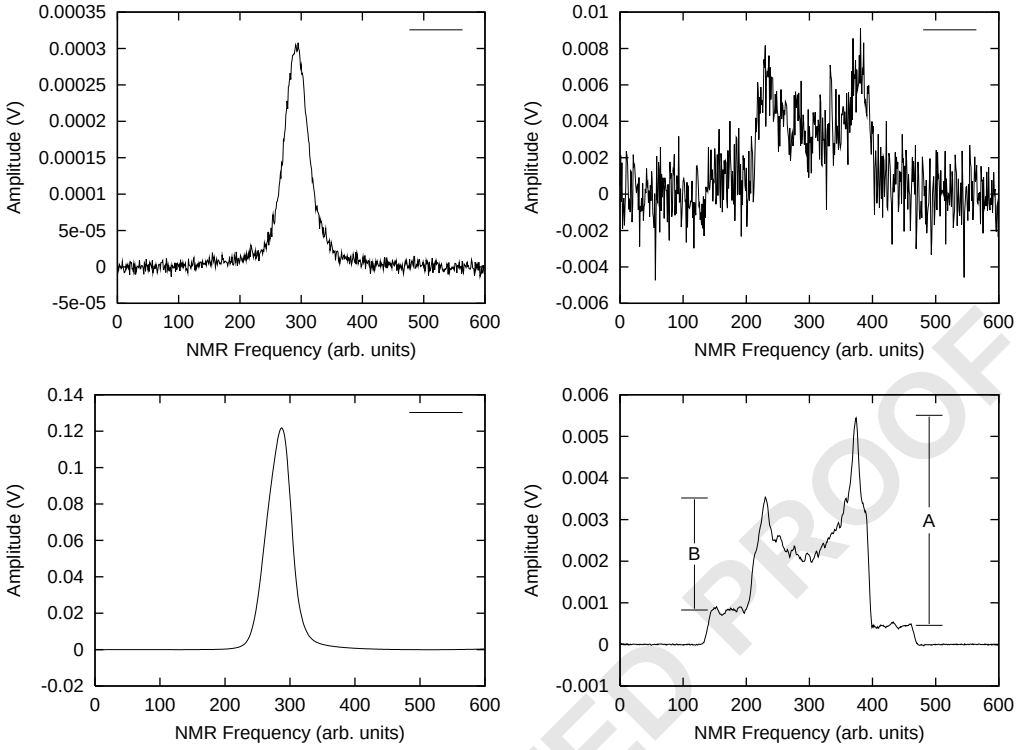

Fig. 6. Typical NMR signals for NH_3 (left) and ND_3 (right). Thermal equilibrium (TE) signals are shown at the top and enhanced polarization signals at the bottom. All signals are the result of 5000 double frequency sweeps as described in the text. The ND_3 TE signal is the sum of 10 sets of 5000 double sweeps. The transition strengths A and B can be used to estimate the deuteron vector polarization. Details in the text.

provide a precise value of the target polarization, with accuracy of the order of 3–4%, even using small data samples recorded in a few hours. Moreover, the method described below samples only the portion of the target illuminated by the electron beam, and thus avoids problems associated with nonuniformities in the target polarization.

The longitudinal analyzing power for elastic scattering can be written as [12]

$$A_{\parallel} = \sqrt{1-\varepsilon^2}\cos\theta_{\gamma}\,\frac{A_1+\eta A_2}{1+\varepsilon R}. \tag{2}$$

Here θ_{γ} is the angle between the exchanged virtual photon and the target spin, ε is the photon polarization, A_1 and A_2 are well-known functions of the electric and magnetic nucleon form factors, R is the longitudinal–transverse cross-section ratio σ_L/σ_T, and $\eta = \sqrt{2\varepsilon/(1+\varepsilon)}\tan\theta_{\gamma}$. This asymmetry can be calculated for both protons and neutrons from known nucleon form factors with very little systematic uncertainty (less than 1–2% in our kinematic region).

The corresponding raw scattering asymmetry for a target polarized parallel to the beam direction is

$$A = \frac{N^{\Uparrow\downarrow} - N^{\Uparrow\uparrow}}{N^{\Uparrow\downarrow} + + N^{\Uparrow\uparrow}} \tag{3}$$

$$= f P_b P_t A_{\parallel}. \tag{4}$$

Here N represents the number of polarized electrons scattered elastically (quasi-elastically) by a polarized proton (deuteron) target. The $\Uparrow$ and $\uparrow$ arrows indicate the target and beam spin orientations, respectively. P_b and P_t are the beam and target polarizations, and f is the target dilution factor, defined as the ratio of electrons scattered from polarizable nucleons to the total number of scattered electrons.

The above relation can be used to extract the product $P_b P_t$ and hence P_t, once P_b has been measured via Møller polarimetry. The dilution factor can be determined by comparison of detector yields between a polarized sample and a carbon (or nitrogen) sample of known density and thickness. Further details can be found in Ref. [13].

The deuteron polarization is extracted from beam asymmetries using inclusive quasi-elastic $d(e, e')$ events in the range $0.85\ \text{GeV} \leqslant W \leqslant 1.0\ \text{GeV}$. We use a simulated deuteron wave function [14] to calculate the expected analyzing power $A_{\|}$ for inclusive quasi-elastic scattering within our kinematic cuts, which differs only slightly from the cross-section-weighted average of the proton and neutron asymmetries.

A comparison between this technique and the NMR measurements described above is shown in Fig. 7. Each run corresponds to approximately 2 h of data with a beam current of 3 nA. The proton target was annealed just prior to the first data point. As can be seen in the figure, the initial data points are in close agreement with one another, but the NMR results decay less rapidly in subsequent measurements. A second anneal was done prior to run 28565, and the results come into temporary agreement once more.

This discrepancy can be explained by the fact that the NMR and scattering asymmetries were effectively sampling different portions of the target. To ensure that the electron beam did not strike the outer edges of the sample container, the beam was not rastered over the full 15 mm diameter of the target, but instead over a 12 mm diameter at the center. Thus only this portion was depolarized by beam-induced radiation damage. The NMR coil, wrapped around the outside of the sample container, was primarily sensitive to the polarization of material outside the beam spot, and so reported an erroneously large value of P_t. Annealing the target repairs most of the beam-induced radiation damage, after which the polarization inside the beam spot becomes equal to that outside. These results clearly demonstrate the importance, when possible, of using the incident beam to determine the target polarization.

3.7. Control software

Two software systems operating on separate computers are used to monitor and control the polarized target. One system is primarily dedicated to the NMR measurements, while the second is used to control the various cryogenic subsystems. Communication between the two software systems is possible, so data may be passed from the NMR

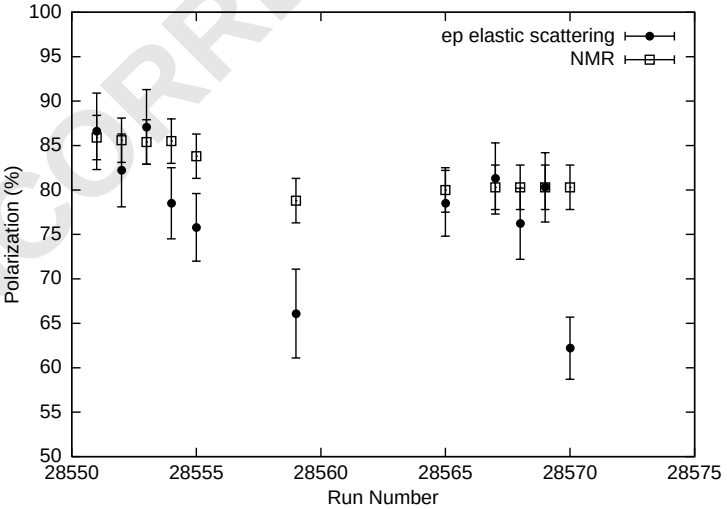

Fig. 7. Comparison of the proton polarization determined using the NMR and elastic scattering techniques described in the text. Each run consists of approximately 2 h of data acquired with a beam current of 3 nA.

to the cryogenic control computer as needed. This division of labor between two software systems provides very robust and flexible control of the polarized target.

The NMR data acquisition system software is Labview 5.2[11] which operates on a PC located in the experimental hall. The primary function of this software is the control of the RF oscillator frequency and the acquisition of the NMR signal. It is also used to control the superconducting magnet, the microwave oscillator, and target insert motion. A client–host connection is established between this and a second PC, located in the counting house, to allow constant user access to the NMR controls.

The cryogenic systems for the target are controlled by the Experimental Physics and Industrial Control Software (Epics). This software runs on a VME-based single board computer in the experimental hall. Most processes are handled automatically by the software, with alarm levels established to warn the user in case of a potential problem. Examples include the periodic filling of the superconducting magnet's reservoir, and the operation of the refrigerator's needle valve to maintain a constant level of LHe within the evaporation chamber. The single board computer is connected to the Jefferson Lab Local Area Network and a graphical user interface for the control software may be accessed from any Unix/Linux workstation on site.

4. System performance

The polarized target was operated in CLAS for two separate run cycles, the first lasting 3 months in 1998, and the second 7 months during 2000–2001. Numerous changes to the target were made during the 18-month period between the cycles to improve the performance of the target as well as its reliability. These changes included a new data acquisition system for the NMR, modifications to the insert lifting mechanism, an increase in microwave power delivered to the target, an increase in refrigerator pumping speed, and improved diagnostic instrumentation. In its final configuration, the target operated in a very reliable manner. Most processes were fully automated so that the target could operate continuously for several days with almost no user intervention. Exceptions included the occasional polarization reversal and annealing of target material.

During the first run cycle typical proton and deuteron polarizations, based on the NMR measurements, were 69% and 20%, respectively. Following the improvements mentioned above, the typical values improved to 74% for the proton, and 35% for the deuteron. Maximum proton and deuteron polarizations achieved were 96% and 46%, respectively. The polarization history for a series of 1000 consecutive runs (about 2000 h) during the second experimental cycle is shown in Fig. 8. Positive and negative polarizations for both the NH_3 and ND_3 target are shown in the figure. Periodic polarization reversals and target changes are apparent in the figure. Background measurements taken with the carbon and empty targets are not indicated.

Typical electron beam currents encountered during the EG1 series of experiments were 1–6 nA, limited by the maximum counting rate for the CLAS detector. With this beam current, target anneals were necessary about once a week, and no beam-heating effects on the target polarizations were observed.

5. Summary

We have described the design, operation, and performance of a polarized target of protons and deuterons suitable for use inside a large, 4π spectrometer. Protons and deuterons in paramagnetically doped $^{15}NH_3$ and $^{15}ND_3$ were continuously polarized by microwave irradiation at a temperature of 1 K and a magnetic field of 5 T. The target has produced proton and deuteron polarizations as high as 96% and 46%, respectively. To our knowledge this is the first polarized target to operate inside a large acceptance detector while permitting the rapid selection from multiple target samples.

[11] National Instruments Corp., Austin, TX.

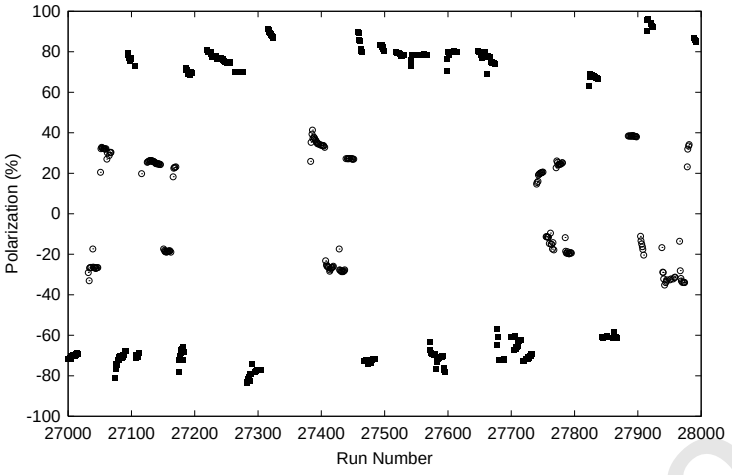

Fig. 8. Polarization history (NMR values) of both the NH_3 target (■) and ND_3 target (⊙) over the course of approximately 2000 h. Both positive and negative polarizations are plotted. Runs utilizing either the carbon target or empty cell are not indicated.

The novel design of this target resulted from the unusual geometry constraints of the CLAS detector and the need to service a wide ranging experimental program. We have described the impacts this design has had on the ultimate performance of the target, notably its elevated helium consumption and reduced cooling power. Nevertheless, it has proven very successful in its role as a general purpose polarized target for a 4π spectrometer.

We have observed discrepancies in target polarization values extracted using traditional NMR methods and from elastic scattering asymmetries. The discrepancies result from radiation damage from the electron beam coupled with an undersized beamspot on the target.

Acknowledgements

The authors gratefully acknowledge the expert support provided by the technical staffs of the Jefferson Lab Target Group, Jefferson Lab Hall B, University of Virginia Physics Department, and INFN-Genova. We also benefitted from fruitful discussions with Professor Werner Meyer of the Ruhr Universität–Bochum. This work was supported in part by grants from the United States Department of Energy and the National Science Foundation, and by an Academic Enhancement Program grant from the University of Virginia.

References

[1] B.W. Filippone, X.D. Ji, hep-ph/0101224, 2001.
[2] J. Ahrens, et al., Phys. Rev. Lett. 87 (2001) 022003.
[3] G. Anton, in: S. Simula, B. Saghai, N. Mukhopadhhyay, V. Burkert (Eds.), Few Body Systems, Springer, Berlin, 1998, p. 177 Proceedings of the Workshop on N^* Physics and Non-perturbative QCD, Trento, Italy.
[4] A. Abragam, M. Goldman, Rep. Prog. Phys. 41 (1978) 396.
[5] D.G. Crabb, W. Meyer, Annu. Rev. Nucl. Part. Sci. 47 (1997) 67.
[6] W. Brooks, et al., Nucl. Phys. A 663 (2000) 1077c.
[7] T.D. Averett, et al., Nucl. Instr. and Meth. A 427 (1999) 440.
[8] P. Roubeau, Cryogenics 6 (1966) 207.
[9] Guy K. White, Experimental Techniques in Low-Temperature Physics, 3rd Edition, Clarendon Press, Oxford.
[10] G.R. Court, D.W. Gifford, P. Harrison, W.G. Heyes, M.A. Houlden, Nucl. Instr. and Meth. A 324 (1993) 433.
[11] K. Guckelsberger, F. Udo, Nucl. Instr. and Meth. 137 (1976) 415.
[12] A. Bartl, W. Majerotto, Nucl. Phys. B 62 (1973) 267.
[13] M. Anghinolfi, et al., CLAS-note 00-01: measure of target and beam polarization in EG1 data, http://www.jlab.org/Hall-B/notes/clas_notes00/00-001.ps, 2000.
[14] M. Lacombe, et al., Phys. Rev. C 21 (1980) 861.